ISTITUTO NAZIONALE DI FISICA NUCLEARE

Sezione di Genova

INFN/BE-85/4
15 Ottobre 1985

E. Di Salvo: SEMICLASSICAL SCATTERING THEORY: NUCLEAR ELASTIC SCATTERING

Servizio Documentazione
dei Laboratori Nazionali di Frascati

Istituto Nazionale di Fisica Nucleare
Sezione di Genova

INFN/BE-85/4
15 Ottobre 1985

SEMICLASSICAL SCATTERING THEORY: NUCLEAR ELASTIC SCATTERING

E. Di Salvo
Dipartimento di Fisica dell'Università, Genova
INFN, Sezione di Genova, Genova

ABSTRACT

We intend to wrute the semiclassical scattering amplitude as a sum of terms, each of them being associated to a trajectory. First of all we study the classical equations of motion, considering both the analytical (real and complex) solutions and a certain type of singular solutions, which behave similarly to the diffracted rays in optics; in particular, in the case of a central nuclear potential, we single out classical effects like rainbow and orbiting and also wave effects like diffraction and direct reflection. Successively, considering the Debye expansion of the scattering amplitude relative to a central nuclear potential, and evaluating asymptotically each term by means of the saddle point technique, we determine the decay exponents and diffraction coefficients relative to such a potential.

RIASSUNTO

Intendiamo scrivere l'ampiezza di diffusione semiclassica come somma di termini, ciascuno dei quali è associato ad una traiettoria. Prima di tutto studiamo le equazioni classiche del moto, considerando sia le soluzioni analitiche (reali e complesse) sia un certo tipo di soluzioni singolari, che si comportano in modo simile ai raggi diffrattati in ottica; in particolare, nel caso di un potenziale nucleare centrale, isoliamo effetti classici, come l'arcobaleno e la spiralizzazione, ed anche effetti ondulatori come la diffrazione e la riflessione diretta. Successivamente, considerando l'espansione di Debye dell'ampiezza di diffusione relative ad un potenziale nucleare centrale, e valutando asintoticamente ciascun termine per mezzo della tecnica del punto a sella, determiniamo gli esponenti di decadimento ed i coefficienti di diffrazione relativi a tale potenziale.

1. Introduction

As is well-known, the usual WKB approximation fails when one considers the scattering due to an absorptive and/or rapidly varying potential. Knoll and Schaeffer[1] overcome this difficulty by considering not only real solutions of the classical equations of motion, but also some of the complex ones (see also the numerous references quoted in [1]); in this approach the scattering amplitude is expressed as a sum of terms, each of them being interpretable as a contribution from a given (real or complex) trajectory. Unfortunately, in the case of a transparent or weakly absorbing potential, this method does not apply when one considers trajectories with angular momenta close to the orbiting angular momentum, since the WKB phase shift has a branch point. On the contrary Brink and Takigawa[2] extend the semiclassical solution of the three turning point scattering problem[3] to the case of a complex potential, obtaining an approximate scattering amplitude which is suitable also in the case of a transparent (or weakly absorbing) potential; however such a scattering amplitude is not directly interpretable in terms of trajectories, since it is expressed as a partial-wave series.

One of the purposes of this paper is to fill such a gap, showing that, in the limit of $\hbar \to 0$, it is generally possible to decompose the scattering amplitude into contributions from trajectories. Such a decomposition, of course, shortens numerical calculations, but it is also interesting in itself, since it has an immediate physical interpretation; in particular, as we shall see, one singles out classical effects like rainbow and orbiting[4], and also diffractive effects like surface waves[5],[6],[7]: these

last behave in a wholly similar way to those which are excited at the edge of a transparent sphere in optics[8].

Our treatment, which is similar to those by Levy and Keller[9] and by Nussenzveig[8] in optics, is developed in two steps:

i)Firstly, in the case of a rather general analytical potential, one analyses the branches of the solution of the Hamilton-Jacobi equation: besides the analytical ones - both real and complex[1] - one considers certain singular branches[3]. The wavefunction - and therefore the scattering amplitude - results in a sum over these branches. At this stage the theory contains heuristic elements, in the sense that some proportionality contants, like diffraction coefficients and decay exponents, are left undetermined.

ii)Secondly, starting from the approximate expression of the partial-wave amplitude deduced in ref.[2], one writes the scattering amplitude relative to a central potential as a series of integrals thanks to Poisson's sum formula; moreover the Debye expansion of the scattering amplitude is performed, similarly to ref.[8] (see also[10]). Each term of this expansion is evaluated asymptotically for $\hbar \to 0$ by means of the saddle-point technique: the main contributions come from saddle points (which correspond to analytical trajectories) and from poles (which represent the contribution of the singular trajectories). The decay exponents and diffraction coefficients, as well as the other proportionality constants, are determined by comparing the asymptotic expression of the pole contribution with the term relative to the singular trajectories, found in step i).

In particular our treatment explains the difference between orbiting and surface waves, two effects which, however, result to be very similar and are intimately

connected in the case of an analytical potential; more precisely both these two terms represent waves which decay exponentially in the direction of propagation, with the same decay constant (sect. 4). Furthermore the surface waves are found to propagate not only from the lit region to the shadow region, but also in the opposite sense: this effect, which was illustrated mathematically by Nussenzveig[8] in the case of scattering by a sharp-edged sphere, turns out to be present also in the case of a smooth, transparent potential.

The surface-trajectory contributions play an important role in explaining large-angle peaks in nuclear and heavy-ion elastic scattering[5],[6]: in this sense our theory provides a link between the traditional optical model, which is commonly used for analysing the scattering data, and the geometrical theory of diffraction, which was used phenomenologically for interpreting ALAS[5]. Even though in the present paper we refer mainly to nuclear potentials, our treatment has a much more general validity, mainly in the first step, as we have already seen; in particular the effects now described could be singled out also with other potentials, like, e.g., the atomic ones, even though in this case also other effects, like hard-core repulsion, should be taken into account.

The paper is organized as follows. In sect.2 we develop the first step of our theory, i.e., we write the scattering amplitude (relative to a real potential) as a sum over contributions from analytical and singular trajectories. Sect.3 is devoted to the second step, i.e. to the Debye expansion and to the asymptotic evaluation of the scattering amplitude. In sect.4 we make some remarks on particular effects, like resonances, orbiting and surface

waves; moreover we consider shortly the effects of absorption and we outline some possible developments of the present theory. Lastly in the appendix we prove some results which we use in sect. 3.

2. Hamilton-Jacobi equation and transport equation

In this section we are mainly concerned with a description of the (real and complex) trajectories involved in an elastic scattering process; the wavefunction - and consequently the scattering amplitude - is written as a sum of contributions from each trajectory. Firstly (subsect. 2.1) we treat a generic potential, then (subsect. 2.2) we specialize our considerations to the case of a central (nuclear) potential.

2.1. General theory

The stationary Schrödinger equation for a spinless particle of mass μ scattered by a potential $V(\vec{r})$ reads as

(2.1) $H(\vec{P},\vec{r})\psi(\vec{r})=E\psi(\vec{r})$,

where

(2.2) $H(\vec{P},\vec{r})=\frac{\vec{P}^2}{2\mu}+V(\vec{r})$

and $\vec{P}$ is the momentum operator. We assume $V(\vec{r})$ to consist in two terms, i.e.,

(2.3) $V(\vec{r})=V_o(\vec{r})+U(\vec{r})$,

where, for large values of $r=|\vec{r}|$, $V_o(\vec{r})=o(\frac{1}{r})$ and $U(\vec{r})\cong\frac{2\eta E}{kr}$, η being the Sommerfeld parameter and $\hbar k=\sqrt{2\mu E}$; both potentials in (2.3) are local, real-valued and C^∞ throughout all $\vec{r}$-space.

Since we are interested in a scattering problem, we impose $\psi(\vec{r})$ to satisfy, for large values of r, the outgoing-wave boundary condition; in particular the

unscattered wave is characterized by an incident momentum $\hbar\vec{k}$, such that $|\vec{k}|=k$.

We assume the potential to vary slowly with respect to a displacement of the order of the De Broglie wavelength, except, at most, on a finite number of thin layers located in neighborhoods of certain smooth surfaces, which we call Ξ_i $(i=1,2...n)$; the location of these surfaces will be stated more precisely below. Then a convenient choice of the trial solution of eq. (2.1) in the limit of $\hbar\to 0$ has been shown to be[11]

(2.4) $\psi(\vec{r})=\sum_\nu a_\nu g_\nu \exp(iW_\nu/\hbar)$,

where g_ν and W_ν are chosen so as to fulfill, respectively, the Hamilton-Jacobi and the transport equation, i.e.,

(2.5) $H(\vec{\nabla}W_\nu,\vec{r})=E$,

(2.6) $\vec{\nabla}\cdot(g_\nu^2\vec{\nabla}W_\nu)=0$;

then the Schrödinger equation will be satisfied if

(2.7) $\frac{2}{\mu}g_\nu\vec{\nabla}W_\nu\cdot\vec{\nabla}a_\nu=i\hbar\Delta(a_\nu g_\nu)$.

Let us examine the equations (2.5) to (2.7) in some detail.

2.1.1. Hamilton-Jacobi equation.

In order to fulfill the outgoing-wave boundary condition, the function W, which appears in (2.5), must coincide, on a plane Σ_o perpendicular to $\vec{k}$ and located at large distance from the origin of the reference frame, with the phase of the unscattered Coulomb wavefunction; furthermore the vector $\vec{k}$ must be directed towards the interaction region. Let us consider the Hamiltonian characteristic system associated with the partial differential equation (2.5), i.e.,

(2.8) $\vec{\nabla}_p H=d\vec{r}/ds$, $\vec{\nabla}_r H=-d\vec{p}/ds$, $dW/ds=\vec{p}\cdot d\vec{r}/ds$,

where we have set

(2.8') $\vec{p}=\vec{\nabla}W$

and s is a parameter along the characteristics. We impose

that for s=0

(2.9) $\vec{r}\in\Sigma_o$, $\vec{p}=\hbar\vec{k}$.

Let us introduce two real parameters, σ_1 and σ_2, in order to characterize the points of the plane Σ_o. Then, if we consider any compact set in the space $\vec{R}=(\sigma_1,\sigma_2,s)$, the system (2.8) has one and only one C^∞ real-valued solution for each couple of values of σ_1 and σ_2, i.e.,

(2.10) $\vec{r}=\vec{r}(\sigma_1,\sigma_2,s)$, $\vec{p}=\vec{p}(\sigma_1,\sigma_2,s)$, $W=W(k,\sigma_1,\sigma_2,s)$.

A well-known theorem[12] guarantees that (2.10) provides the solution of the Hamilton-Jacobi equation if and only if the Jacobian determinant

(2.11) $J=\partial(x,y,z)/\partial(\sigma_1,\sigma_2,s)$, $\vec{r}\equiv(x,y,z)$,

is finite and does not vanish. Generally this condition is not fulfilled throughout the whole space. The set of points where the Jacobian (2.11) vanishes constitutes the caustic; the solution of the Hamilton-Jacobi equation results to be many-valued, the branch-points being the points of the caustic, and the sum (2.4) is made to run over all the branches of W at each point of the space.

Furthermore the caustic delimitates the so-called classically forbidden regions (or shadow regions, as opposed to the lit regions, where the classical trajectories, i.e., the real-valued characteristics, can arrive): if the potential is analytic, (2.10) can be continued analytically for complex values of the coordinates and of the parameters σ_1, σ_2, s, allowing us to extend to such regions the semiclassical description of the wavefunction by means of complex characteristics (see [1],[9],[11]; [3] and references quoted therein). We note that, because of the Schwartz reflection principle, if $\vec{r}(\sigma_1,\sigma_2,s)$ is a solution of (2.8), obtained as an analytical continuation of (2.10), also $\vec{r}(\sigma_1^*,\sigma_2^*,s^*)=\vec{r}^*(\sigma_1,\sigma_2,s)$ is a solution; therefore one is faced with the delicate problem of the correct analytical

continuation into the shadow region: as we shall see in detail in the next section, the correct trajectory is the one which gives an exponentially small contribution to the wavefunction. As we shall see in a moment, the extension to complex trajectories implies the inclusion of further branches of W in the sum (2.4).

The Jacobian (2.11) relative to the mapping $\vec{R}\to\vec{r}$ may diverge on certain surfaces in the $\vec{r}$-space, in correspondence of certain couples of the parameters σ_1, σ_2, such that the characteristic $\vec{r}(\sigma_1,\sigma_2,s)$ is grazing to those surfaces in the limit of $s\longrightarrow\infty$; since this is due to the rapid variaton of the potential, it seems natural to identify such surfaces with the above mentioned surfaces Ξ_i. Such singularities in the mapping $\vec{R}\to\vec{r}$ imply that we must take into account further branches of W: these can be exhibited if we extend our investigation to complex characteristics (different from those obtained by anlytical continuation of real characteristics) and to singular characteristics, i.e., not belonging to C^∞ [3]; obviously the index ν in (2.4) must be made to run over all such branches. As regards the complex trajectories, these are caused by classical trajectories which incide on a surface Ξ_i at a non-grazing angle: direct reflection is described (if the potential does not vary too rapidly) by a complex trajectory whose turning point(*) is located near the surface [3],[11],[13]. Owing to the multivaluedness of the above mentioned mapping, it is convenient to subdivide the analytical trajectories into classes, such that for each

---

(*) Here by turning point we mean the point in the (complex) $\vec{r}$-space for which the component of $\vec{p}(\sigma_1,\sigma_2,s)$ normal to Ξ_i vanishes.

class the mapping is single-valued; the inverse mapping may be still many-valued, giving rise, for each class of trajectories, to a caustic surface[11]. Also for these trajectories a problem of analytical continuation arises, since, if $\vec{r}_o$ is a turning point, also $\vec{r}_o^*$ is a turning point; the choice of the right trajectory must be made according to the rule stated above about the analytical continuation to complex trajectories.

Lastly, when a trajectory grazes a surface Ξ_i, singular trajectories must be considered[3], as in the geometrical theory of diffraction[9]; such trajectories consist in two branches of classical trajectory tangent to Ξ_i at two points Q_o and Q, joined smoothly by an arc of geodesic on Ξ_i which has at Q_o and Q the same tangent of the grazing trajectories. The surface trajectory undergoes, at each point on Ξ_i, a splitting into two or more branches, one continuing along the surface, while the remaining ones leave Ξ_i tangentially. Rigorously speaking, in this case, when we say classical trajectories, we mean trajectories not in the crudest semiclassical sense, but smoothed off by barrier penetration effects; this question will be explained more extensively in the next section.

Let us conclude this paragraph with an observation. The singular trajectories could be taken into account at each point in space, but, as we shall see at 2.1.3., they do not give a significant contribution outside Ξ_i; in any case, inclusion of singular trajectories also at points where the potential varies smoothly would permit us to consider a more general approximation than the one made in this section[3],[11].

2.1.2. Transport equation

Equation (2.6) is solved by

(2.12) $q=J^{-\frac{1}{2}}$,

where J is given by (2.11). The branch of the square root to be chosen depends on the right analytical continuation across the points of the caustic[1],[5](3rd paper); such a continuation has to be made in such a way that, in passing through classically forbidden regions, the function W acquire a positive imaginary part, in accord with the connection rule stated in the preceding paragraph. As a result, every time a characteristic crosses a focal point, the phase of the wavefunction undergoes a jump of $-m\pi/2$, where m is the order of the zero of the Jacobian (2.11) at that point.

2.1.3. Behavior of the coefficients a_ν.

As can be seen from (2.7), the functions a_ν can be approximated by constants if the q_ν are slowly varying. This condition is not fulfilled if we are near a caustic (as can be checked from eq.(2.12)) or if the potential is rapidly varying (as one can easily argue from equations (2.5) and (2.6)). Therefore the space results to be subdivided into regions, separated from one another by sheets of the caustic or by the small layers near Ξ_i, where the potential varies rapidly; within each region the a_ν can be approximated by constants, but in the transition from a region to another they have sudden variations, like Stokes' multipliers[11]. In particular let us analyse in some detail the behavior of the a_ν on Ξ_i. On these surfaces the rapid variation of a_ν is due to the splitting of the trajectories into two or more branches: for trajectories which do not graze Ξ_i the splitting is described by complex turning points, as we have seen. On the other hand, as regards the grazing trajectories, we assume, at each point of the surface Ξ_i, the amplitude along the outgoing trajectory to be proportional to the amplitude along the

incoming trajectory, through a coefficient which depends, approximately in the limit of $\hbar \to 0$, on the local properties of the surface; consequently the amplitude along the surface trajectory undergoes at each point an attenuation proportional to the amplitude itself and to the length of the infinitesimal arc of geodesic described; therefore on Ξ_i we assume that

$$a_\nu \propto \exp\left[-\int \alpha(\zeta)\, d\zeta\right],$$

where $\alpha(\zeta)$ is a complex coefficient, called decay exponent, which depends, again, approximately on the local properties of the surface. All these proportionality coefficients, which have been introduced heuristically, will be determined in the next section in the case of a central potential. Lastly let us observe that, since in the regions where the potential varies smoothly the coefficients a_ν can be regarded as constants, the probability current density associated to each addend of (2.4) is conserved along the "classical" trajectories, so that the current density along the singular paths is negligible.

2.2. Case of a central nuclear potential.

Now let us specialize ourselves to the case of an analytical, central, local potential, consisting in two terms of the type (2.3), one repulsive and slowly varying (electrostatic, $U(r)$) and the other attractive (nuclear, $V_0(r)$): the latter term is rapidly varying at the edge of the nuclear-interaction region, furthermore it is assumed to be purely real, even though our considerations could be extended to the case of a complex potential (see sect. 4). In this case, due to the symmetry of the problem, we take the scattering centre as the origin of the reference frame, the z-axis in the direction of $\vec{k}$ and the parameters σ_1 and σ_2 so as to coincide, respectively, with the angular

momentum, λ and with the azimuthal angle; moreover the polar angle ϑ is the scattering angle. Let us consider a sufficiently low incident energy, so as to have orbiting in correspondence of a given (energy dependent) angular momentum, to be called λ_{12} (a more precise condition will be stated in the next section). Moreover, in order to simplify our theory, we assume the radial momentum, i.e.,

$$p_r = \sqrt{2\mu[E - V_{eff}(r)]}, \qquad V_{eff}(r) = V(r) + \frac{\hbar^2 \lambda^2}{2\mu r^2}$$

to have three and only three turning points for each value of λ; such turning points will be called r_1, r_2, r_3, according to the convention of ref.[2].

As we have already seen in the general theory (subsect. 2.1.1.), in the study of the solution of the Hamilton-Jacobi equation it is necessary to single out the surfaces Ξ_i (if any) where the potential varies rapidly and to subdivide the characteristics into classes. In our case the Jacobian (2.11) becomes infinite on the orbiting sphere, i.e. on the sphere centred at the origin and with a radius equal to the orbiting radius r_{12}; therefore we identify the orbiting sphere with the surface Ξ_1. The first class of analytical trajectories, which we call $K_0^{(a)}$, is constituted by the real analytical trajectories with angular momentum greater than λ_{12}; these trajectories may be either of "Coulomb" type (C.T.) or of "nuclear" type (N.T.)[1], according as the repulsive action (at higher angular momenta) or the nuclear attraction (at lower angular momenta) prevails; the "nuclear" trajectories undergo a negative deflection which increases in modulus for λ approaching λ_{12}. The trajectories of this class form a caustic surface, which we call C_0: this includes the rainbow trajectory (see fig.1 of [11]), i.e., a trajectory of angular momentum λ_r, which, for $r \to \infty$, goes into the direction corresponding to an angle $\vartheta = \vartheta_r$, called rainbow angle.

A second class of analytical trajectories, which we call $K_0^{(b)}$, includes complex trajectories such that $Re\lambda < \lambda_{12}$; some of these, with $Re\lambda$ slightly less than λ_{12}, undergo a negative deflection which, again, increases for λ approaching λ_{12}; the remaining ones are directly reflected at Ξ_1 and undergo a positive deflection. It is worth making an observation as regards the trajectories with $\lambda \cong \lambda_{12}$: in the crudest semiclassical approximation the deflection function would diverge logarithmically at $\lambda = \lambda_{12}$, however, as we shall see in the next section, it is smoothed off by barrier penetration effects[4], so that it has a minimum, say $-\vartheta_0$ ($\vartheta_0 > 0$), near λ_{12}: in this sense orbiting behaves similarly to rainbow[4].

Let us consider other classes of trajectories. $K_1^{(a)}$ is defined as the class of real-valued trajectories with an angular momentum less than λ_{12}: these penetrate inside Ξ_1 and go directly out of it, without undergoing any internal reflections inside the orbiting sphere. Similarly we define $K_p^{(a)}$ as the classes of trajectories with a complex angular momentum, such that $Re\lambda < \lambda_{12}$, which undergo p-1 internal reflections inside Ξ_1. Each class of trajectories $K_p^{(a)}$, for $p \geq 1$, forms a caustic surface, C_p, which is axially symmetric around the z-axis. Another class, defined as $K_0^{(c)}$, includes the trajectories which propagate into the dark side of the rainbow: these trajectories have a complex angular momentum whose real part is nearly equal to λ_R and a negative imaginary part. Then we define as $K_p^{(b)}$, $p \geq 1$, the classes of trajectories which penetrate into the shadow region of the caustic surface C_0 and re-emerge into the lit region of C_p, undergoing p-1 internal reflections inside Ξ_1.

Now let us consider the singular trajectories; we may distnguish some categories. We call Z_0 the category of

those trajectories which consist solely in an arc of geodesic on Ξ_1 which joins smoothly two branches of "classical" trajectory (of angular momentum λ_{12}). Moreover we define Z_1 the set of the trajectories which, besides describing one or two arcs of geodesics on Ξ_1, take one shortcut, i.e. a branch of "classical" trajectory which penetrates inside Ξ_1 and re-emerges tangentially to this sphere. Similarly we define Z_p as the set of singular trajectories which take p shortcuts inside Ξ_1; for $p\geq 2$ the shortcuts may have 0,1,...p-1 internal reflections. Also other categories of singular trajectories are worth being mentioned, i.e., those which are generated by the complex trajectory of (real) angular momentum λ_{23} such that the turning points r_2 and r_3 coincide (we call Ξ_2 the complex extension of the surface of the sphere of radius $r_{23}=r_2=r_3$): each category of these singular trajectories propagates along Ξ_2, moving from the lit region to the shadow region of each caustic surface C_p, $p\geq 1$. Even though these trajectories do not give a significant contribution to the scattering amplitude, they are of some conceptual importance, since they behave similarly to those singled out by Nussenzveig in the case of a sharp-edged sphere[8].

Now we are able to write the wavefunction (2.4) at any point, by determining the functions W_ν and g_ν for any class K_p of analytical trajectories and for any set of singular trajectories; moreover on Ξ_1 we take into account the assumption made in 2.1.3 about the coefficients a_ν. In particular we are interested in the behavior of the wavefunction for very large distances from the origin, whence we deduce the scattering amplitude. This last can be divided into two terms:

(2.13) $f(K,\vartheta)=f_{cl}(K,\vartheta)+f_s(K,\vartheta)$,

where the former addend is the contribution of the

analytical trajectories, whereas the latter one comes from the singular trajectories. As regards $f_{C\ell}(K,\vartheta)$, one has (see also[1])

$$(2.14)\quad f_{C\ell}(K,\vartheta)=\frac{-i}{K}\sum_{p=0}^{\infty}(-i)^{p}\sum_{\nu_p}\sqrt{\frac{\lambda_{\nu_p}}{\Theta'_{\nu_p}\sin\Theta_{\nu_p}}}\exp\left\{i\left[2\delta_{\nu_p}(\lambda_{\nu_p})-\lambda_{\nu_p}\Theta_{\nu_p}\right]\right\},$$

where p is the number of internal reflections that a trajectory undergoes inside the orbiting sphere, while ν_p runs over the classes of trajectories corresponding to a fixed p, and

$$(2.15)\quad 2\delta_{\nu_p}(\lambda)=\lim_{r\to\infty}\left[\int_{T_{\nu_p}}\sqrt{\frac{2\mu}{\hbar^2}\left[E-V(r)\right]-\frac{\lambda^2}{r^2}}\,dr-2kr-2\eta\log(2kr)\right]+\lambda\pi,$$

$$(2.16)\quad \Theta_{\nu_p}=2(d\delta/d\lambda)_{\lambda_{\nu_p}},\quad \Theta'_{\nu_p}=2(d^2\delta/d\lambda^2)_{\lambda_{\nu_p}};$$

the angular momenta λ_{ν_p} are roots of the equation

$$(2.17)\quad \Theta_{\nu_p}(\lambda)=\pm\vartheta-2m\pi=\vartheta'_{\pm},$$

where m is any nonnegative integer; furthermore T_{ν_p} denotes the ν_p-th trajectory: one must take into account the change of the Riemann sheet for the integrand of (2.15), whenever a turning point is crossed. Moreover the function $(\sin\Theta_{\nu_p})^{-\frac{1}{2}}$, which appears in formula (2.14), has branchpoints at $\Theta_{\nu_p}=m'\pi$, m' being any integer, and must be continued starting from the interval $[0,\pi]$, taking branch cuts from 0 to $-i\infty$: the analytical continuation across the branchpoints takes into account the number of axial focal points crossed by the trajectory ([1];[5], 3rd paper); similarly the factor $(-i)^p$ describes the crossing of focal points belonging to the caustics C_p. Moreover it is straightforward to see that the series (2.14) converges, since, due to the complex turning points in the multireflection pattern, the p-th term decreases exponentially at increasing p. Lastly let us spend a few words about the roots of eq. (2.17): first of all we must consider all the real roots, which correspond to classes $K_0^{(a)}$ and $K_1^{(a)}$ of the trajectories; as regards the

complex trajectories, we have to keep in mind the connection rule seen in 2.1.1.

Near ϑ_n and $\bar{\vartheta}_o$ (where $\bar{\vartheta}_o = \pm\vartheta_o \pmod{2\pi}$, $0<\bar{\vartheta}_o<\pi$) one has to recur to the uniform approximation[15],[16].

As for the latter addend of (2.14), if we take into account only the surface trajectories on the surface Ξ_1, we have[5]

$$(2.18)\quad f_S(K,\vartheta) = \frac{e^{i\frac{\pi}{4}}}{K}\sum_{m=0}^{\infty}\sum_{m=0}^{\infty}\frac{D_m^2\, e^{i\left[2\,\delta_1(\lambda_{12})+\lambda_{12}\vartheta_o\right]}}{\sqrt{\cos\frac{\vartheta_o}{2}}}\cdot$$

$$\cdot\sum_{p=0}^{\infty} e^{ip\left(\phi-\frac{\pi}{2}\right)}\left\{\frac{e^{i\lambda_m \zeta_{pm}^{+}}\;\mathcal{L}_p\left(\zeta_{pm}^{+}\right)}{\sqrt{\sin\vartheta_+'}}+\frac{e^{i\lambda_m \zeta_{pm}^{-}}\,\mathcal{L}_p\left(\zeta_{pm}^{-}\right)}{\sqrt{\sin\vartheta_-'}}\right\}$$

where

$$(2.19)\qquad \zeta_{pm}^{\pm} = \zeta_p^{\pm} + 2m\pi$$

$$(2.19')\quad \zeta_p^{\pm} = \pm\vartheta - \vartheta_o - p\vartheta_t \pmod{2\pi},\ (0<\zeta_p^{\pm}<2\pi),$$

$$(2.19'')\quad \lambda_m = \lambda_{12} + i\alpha_m\ ,$$

$$(2.19''')\quad \mathcal{L}_p(\zeta_{pm}) = \sum_{j=1}^{p}\binom{p-1}{j-1} R_{22}^{(p-j)}(D_n)^j\,\frac{(\zeta_{pm})^j}{j!},\quad \mathcal{L}_o(\zeta_{om}) = 1;$$

$\vartheta_\pm'$ have been defined by (2.17), furthermore ϑ_t is the angle corresponding to the shortcut, ϕ the classical action along the shortcut; $D_n = D_{12}D_{21}(g_f/g_i)^{1/2}$ is the product of two limiting refractive coefficients by the ratio of two factors of flux([5], 3rd paper), D_n the diffraction coefficients, R_{22} the internal reflection coefficient and α_m the decay exponents; we assume $\mathrm{Re}\,\alpha_m>0$. The values of these proportionality coefficients will be determined in the next section. Lastly $\delta_1(\lambda)$ is given by (2.15), considering the trajectory which has only one turning point, at $r=r_1$.

It is easy to see that the series in p, which appears in (2.18), converges, since in the limit of $\hbar\to 0$ both D_n and

R_{22} are in modulus less than 1, as can be checked from formulae (3.18) and (3.23). Moreover we observe that there are some particular angles, corresponding to the deflection angles $\vartheta' = -\vartheta_0 - p\vartheta_t$, in neighbourhoods of which the approximations (2.18) and (2.19) fail: these are the so-called Fock transition regions[8] and correspond to "limiting" trajectories which constitute a part of the caustic surfaces C_p, $p \geq 1$; near these angles the uniform approximation must be used.

Lastly let us observe that the semiclassical approximation fails in the neighborhood of the axial caustic, i.e., for $\vartheta = 0$ and $\vartheta = \pi$.

3. The Debye expansion of the scattering amplitude.

It has been shown[15], by using the Poisson sum formula and the usual asymptotic expansion of the Legendre functions, that the scattering amplitude can be written as

$$(3.1)\quad f(k,\vartheta) = \sum_{m=-\infty}^{\infty} [f_m^+(k,\vartheta) + f_m^-(k,\vartheta)],$$

with

$$(3.2)\quad f_m^{\pm}(k,\vartheta) = \frac{i(-)^{m+1}}{k\sqrt{2\pi \sin\vartheta}} \int_0^{\infty} \lambda^{1/2} S(\lambda,k) \exp\left\{ i[2\pi m\lambda \pm (\lambda\vartheta - \pi/4)] \right\} d\lambda.$$

The approximation written above fails in a neighborhood of $\vartheta = 0$ and of $\vartheta = \pi$.

Now we use the S-function approximation deduced by Brink and Takigawa[2], i.e.

$$(3.3)\quad S(\lambda,k) = \frac{e^{2i\delta_1}}{N(i\varepsilon)} \left[1 + \frac{e^{-2\pi\varepsilon} e^{2iS_{32}}}{N(i\varepsilon) + e^{2iS_{32}}} \right],$$

where δ_1 is given by (2.15) and

$$(3.3')\quad \varepsilon = \frac{-i}{\pi} A(r_2, r_1), \quad S_{32} = A(r_3, r_2),$$

$$(3.3'')\quad A(r,r') = \int_r^{r'} \left\{ \frac{2\mu}{\hbar^2} [E - V(r)] - (\lambda/r)^2 \right\}^{1/2} dr,$$

r_1 , r_2 , r_3 being the turning points; lastly

$$(3.3'') \quad N(i\varepsilon)=\frac{\sqrt{2\pi}}{\Gamma\left(\frac{1}{2}+i\varepsilon\right)}\exp\left\{i\varepsilon[\log(i\varepsilon)-1]\right\}.$$

This approximation holds true if at $\lambda=\lambda_{12}$ the internal turning point r_3 is sufficiently far from the other two (coincident) turning points.

We show in appendix that (3.3) can be written as a geometric series for any real positive value of λ:

$$(3.4) \quad S(\lambda,k)=\sum_{p=0}^{\infty} S_p(\lambda,k),$$

with

$$(3.4') \quad S_0(\lambda,k)=\frac{e^{2i\delta_1}}{N(i\varepsilon)} \quad , \quad S_p(\lambda,k)=(-)^{p+1}\, e^{-2\pi\varepsilon}\, \frac{e^{2i\delta_1}}{N(i\varepsilon)}\left[\frac{e^{2i\delta_{32}}}{N(i\varepsilon)}\right]^p \quad (p\geq 1);$$

furthermore we show that the series (3.4) can be interchanged with the integral (3.1). As a result we get

$$(3.5) \quad f(k,\vartheta)=\sum_{p=0}^{\infty} f_p(k,\vartheta),$$

with

$$(3.5') \quad f_p(k,\vartheta)=\sum_{m=-\infty}^{\infty}[f_m^{p+}(k,\vartheta)+f_m^{p-}(k,\vartheta)]$$

and

$$(3.5'') \quad f_m^{p\pm}(k,\vartheta)=\frac{(-)^m}{iK\sqrt{2\pi\sin\vartheta}}\int_0^{\infty}\lambda^{1/2}\, S_p(\lambda,k)\exp\left\{i[2\pi m\lambda\pm(\lambda\vartheta-\pi/4)]\right\}d\lambda.$$

The integrand of (3.5'') presents poles of p-th order in the complex λ-plane: the locations of these poles are given by the roots of the equations

$$(3.6) \quad \varepsilon(\lambda)=i\left(n+\tfrac{1}{2}\right), \quad n\geq 0.$$

Now ε is an analytical function for any finite complex value of λ, except at λ_{23}, where it presents a branchpoint; moreover $\varepsilon(\lambda)$ is real for λ real and less than λ_{23}, while for $\lambda>\lambda_{23}$ it presents a nonvanishing imaginary part, corresponding to a branchcut from λ_{23} to $+\infty$; lastly, near λ_{12} one has[2],[4]

$$(3.7) \quad \varepsilon(\lambda)\cong\frac{\hbar\lambda_{12}(\lambda-\lambda_{12})}{r_{12}^2\sqrt{\mu|V_B''|}}$$

where V_B'' is the curvature of the effective potential at $r=r_{12}$. Therefore, using the Cauchy-Riemann relations and the properties of the "isothermal" curves $\{\mathrm{Im}\,\xi=0\}$ and $\{\mathrm{Re}\,\xi=0\}$ in the complex λ-plane, we can show that the poles (3.6) are located, in the first quadrant, on a curve which crosses the real axis at $\lambda=\lambda_{12}$, whereas there are no poles in the fourth quadrant.

3.1 The first term of the Debye expansion.

Let us consider the first term of the series (3.5). To this end it is useful to rewrite the terms of (3.5''), corresponding to p=0, as

$$(3.8)\quad f_m^{o\pm}(k,\vartheta)=\frac{(-)^m}{ik\sqrt{2\pi\sin\vartheta}}\int_0^\infty \lambda^{1/2}\exp\left[i\,\phi_m^{o\pm}(\lambda,\vartheta)\right]d\lambda,$$

with

$$(3.9)\quad \phi_m^{o\pm}(\lambda,\vartheta)=2(\delta_1+m\pi\lambda)\pm(\lambda\vartheta-\pi/4)+i\log[N(i\xi)].$$

The saddle points of integral (3.8) are given by the equation

$$(3.10)\quad \Theta^o(\lambda)=\pm\vartheta-2m\pi=\vartheta_\pm',$$

with

$$(3.10')\quad \Theta^o(\lambda)=2\frac{d\delta_1}{d\lambda}+\varphi_1(\lambda),$$

$$(3.10'')\quad \varphi_1(\lambda)=i\frac{d}{d\lambda}\left\{\log[N(i\xi)]\right\},$$

δ_1 being given by (2.15). Let us study in some detail the deflection function (3.10'). As shown in appendix, $N(i\xi)$ is nearly 1 for any value of λ in the complex λ-half-plane $\mathrm{Re}\,\lambda>0$, except in a neighborhood of the line $\{\mathrm{Re}\,\lambda=0\}$ in the first quadrant (such a region of the complex λ-plane will be called, from now on, H_o); in particular $N(i\xi)$ has a branchpoint at λ_{12}. Therefore, since, as we have seen, $\xi(\lambda)$ has a branchpoint at λ_{23}, $\varphi_1(\lambda)$, as defined by (3.10''), has branchpoints at λ_{12} and λ_{23}: the former one compensates

exactly the orbiting branchpoint at λ_{12} of the WKB deflection function $2\frac{d\delta_1}{d\lambda}$, so that $\Theta^{\circ}(\lambda)$ is analytical at λ_{12}; as for the latter branchpoint, its effects can be neglected in the saddle-point evaluation, since, according to Brink's approximation, λ_{23} is sufficiently far from λ_{12}, therefore $N(i\ell)\cong 1$ in a neighborhood of λ_{23}. Moreover, from the considerations made above it follows that the equation (3.10) corresponds approximately to (2.17), except in a neighborhood of λ_{12}; furthermore, as shown in appendix, $\Theta^{\circ}(\lambda)$ has a negative imaginary part for $\lambda < \lambda_{12}$, while it has a negligibly small imaginary part for $\lambda > \lambda_{12}$. In fig.1 we represent the typical behavior of the real part of $\Theta^{\circ}(\lambda)$, which has a relative maximum, ϑ_r, at λ_r, and a relative minimum, $-\vartheta_o$, close to λ_{12}. Obviously the saddle points to be considered are those in the complex half-plane $Re\lambda>0$, moreover, as we shall see in a moment, these vary both in number and in location according to the value of $\vartheta'_{\pm}$. Furthermore, in order to apply the steepest discent method, one has to deform the path of integration so as to coincide, at least in a neighborhood of the saddle points, with the steepest discent path; in any case, far from the saddle points the integrand of (3.8) must be exponentially small. According to the value of $\vartheta'_{\pm}$, one has to consider five different situations, which we are going to examine in some detail.

i) $0<\vartheta'_{\pm}<\vartheta_r$. In this case we have three saddle points, of which two have a very small imaginary part and a real part greater than λ_{12}; the third one (which corresponds to direct reflection) has a real part less than λ_{12} and a negative imaginary part: this last fact can be shown by observing, from fig. 1, that $Re\{\Theta^{\circ}(\lambda)\}$ has a negative derivative with respect to $Re\lambda$ on the real axis for $\lambda<\lambda_{12}$, and by recalling the Cauchy-Riemann relations and the fact that $Im\,\Theta^{\circ}(\lambda)<0$ on

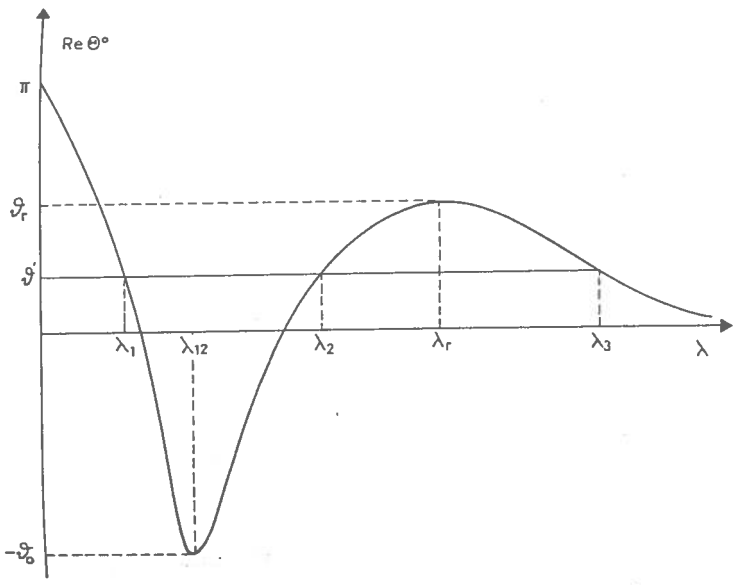

Fig. 1 - The real part of the deflection function $\Theta^{\circ}(\lambda)$ as defined by formula (3.8'). The angles ϑ_r and $-\vartheta_0$ have been defined in subsect. 2.2.

the real axis for $\lambda < \lambda_{12}$. The proper steepest discent path of integration can be determined by observing the behavior of $\mathrm{Re}\,\Phi_m^{\circ\pm\prime} = \mathrm{Re}\,\Theta_0(\lambda) - \vartheta_\pm'$ and recalling still the Cauchy-Riemann relations: the situation is represented in fig. 2a.

ii) $\vartheta_r < \vartheta_\pm' < \pi$. In this case one has still the complex saddle point which corresponds to direct reflection, moreover one has two complex conjugate saddlepoints, such that $\mathrm{Re}\lambda \equiv \lambda_r$; by using arguments very similar to those presented in the case i), one can show that the right saddle point is the one with a negative imaginary part and that the path to be considered is the one represented in fig. 2b; such a saddle point corresponds to a complex trajectory which penetrates into the dark side of the rainbow.

iii) $\vartheta_\pm' > \pi$. In this case only the latter saddle point of ii) needs be considered (see fig. 2c).

iv) $-\vartheta_0 < \vartheta_\pm' < 0$. In this case we have two saddle points, one with a real part slightly less than λ_{12} and with a negative imaginary part, the other with a real part slightly greater

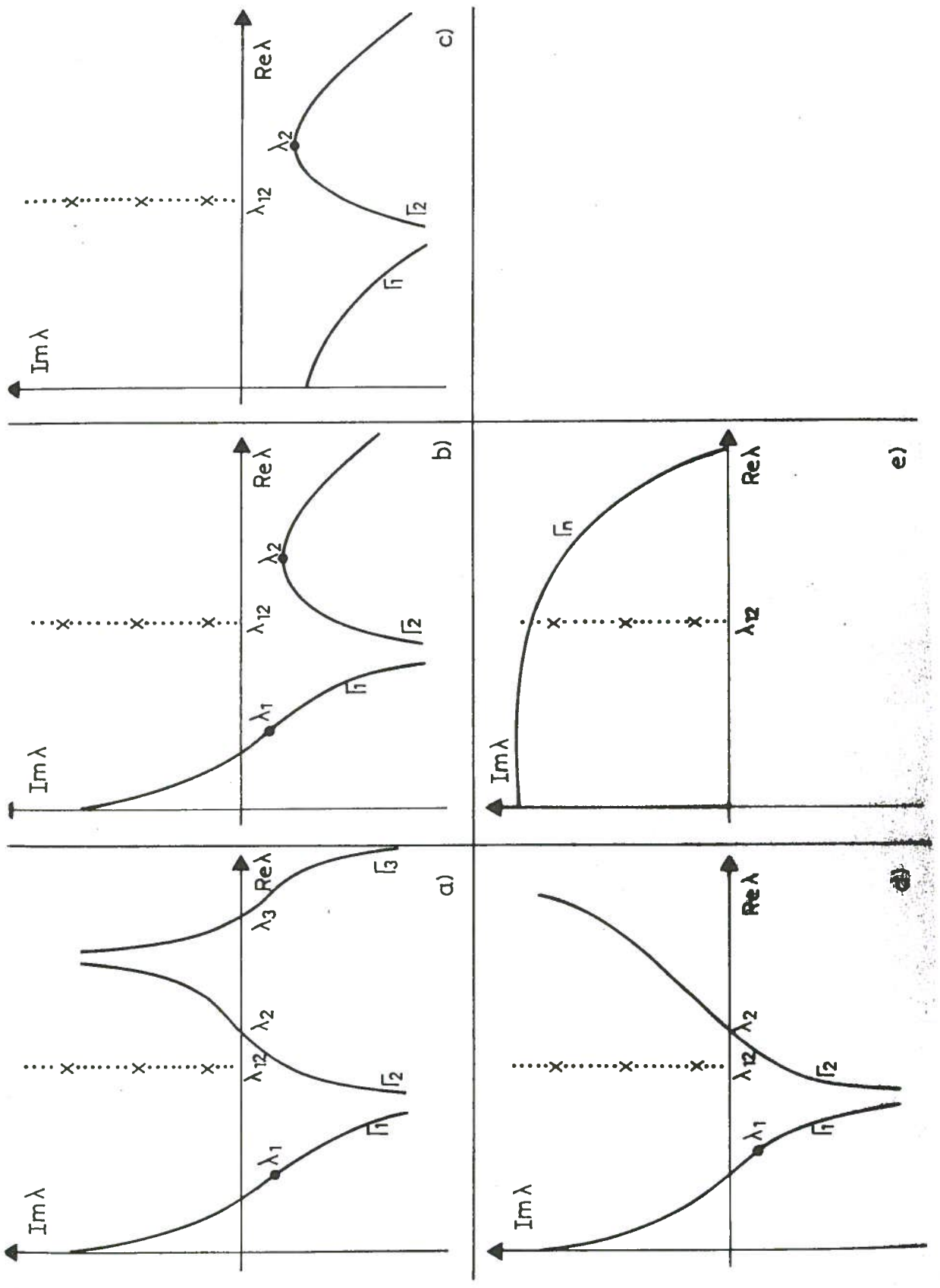

Fig. 2 - Deformation of the path in the integral (3.8) according to the value of (see formula (3.8)): a) $0 < \vartheta'_{\pm} < \vartheta_r$; b) $\vartheta_r < \vartheta'_{\pm} < \pi$; c) $\vartheta'_{\pm} > \pi$; d) $-\vartheta_0 < \vartheta'_{\pm} < 0$; e) $\vartheta'_t < -\vartheta_0$.

than λ_{12}. The paths of integration are represented in fig. 2d.

v) $\vartheta'_{\pm} < -\vartheta_0$. In this situation the equation (3.10) has no roots near the real axis; the roots - which correspond to the values of such that $\phi_m^{o\pm\prime}(\lambda)$ vanishes - lie in the region of the complex λ-plane which we have called H_0; moreover the integrand of (3.8) is exponentially small in the first quadrant, except inside H_0. To see that, let us suppose, for a moment, that φ_1, as defined by (3.10''), would vanish: then we have only two roots of (3.10), which lie very close to λ_{12} (one root is real, such that $\lambda > \lambda_{12}$, the other one is complex, with $\mathrm{Re}\lambda < \lambda_{12}$); moreover, recalling the shape of the WKB deflection function $2\frac{d\delta_1}{d\lambda}$ and the Cauchy-Riemann relations, we conclude that the imaginary part of $\phi_m^{o\pm}(\lambda)$ is positive in the first quadrant and increases at increasing $\mathrm{Im}\lambda$, except in H_0; the presence of the addend φ_1 - which is nearly vanishing in the half-plane $\mathrm{Re}\lambda > 0$ except in H_0 - does not modify substantially the situation, except for pushing such roots into the first quadrant, inside H_0. Therefore in this case it is more convenient to deform the path of integration as in fig. 2e, i.e., choosing a succession of curves Γ_n, which include a part of the positive imaginary axis and an arc in the first quadrant, such that the closed curve constituted by Γ_n and by a segment on the positive real axis encloses the first n poles. From the considerations made above it follows that the integrand of (3.8) is exponentially small along Γ_n, except, at most, in the intersection with H_0; such a difficulty can be overcome if we consider a sufficiently large value of n and let Γ_n pass through the point such that $\xi(\lambda) = i(n+1)$; it can be seen that in these conditions the integrand of (3.8) is exponentially small along Γ_n. Letting n tend to infinity, the integral (3.8) is approximately

equivalent to the series of the residues at the poles in the first quadrant, provided this series converges; the convergence shall be proved in a moment.

Now we are ready to determine the asymptotic behavior of the first term of the Debye expansion. Firstly from the above discussion it follows that for those values of m such that $\vartheta'_{\pm} < -\vartheta_0$ only the residues at the poles must be taken into account, while for the other values of m only the saddle point contributions must be evaluated. Then we have

(3.11) $f_0(k,\vartheta) = f_0^{Sp}(k,\vartheta) + f_0^{Res}(k,\vartheta)$,

where the former term comes from the saddle points, while the latter one comes from the residues. The former term corresponds to the addends with p=0 in the sum (2.15); as for the latter one we have, approximately,

(3.12) $f_0^{Res}(k,\vartheta) = f_{0+}^{Res}(k,\vartheta) + f_{0-}^{Res}(k,\vartheta)$,

with

$$(3.12') \quad f_{0+}^{Res}(K,\vartheta) = \frac{e^{-i\frac{\pi}{4}}}{K\sqrt{\sin\vartheta}}\, e^{i[\Delta_0(\lambda_{12}) + \vartheta_0\lambda_{12}]} \left\{ \sum_{m=m_0}^{\infty} (-)^m \sum_{n=0}^{\infty} \frac{(-)^n\sqrt{\lambda_n}}{n!\,\xi_n}\, e^{i\lambda_n(2\pi m + \vartheta - \vartheta_0)} \right\}$$

and

$$(3.12'') \quad f_{0-}^{Res}(K,\vartheta) = \frac{e^{i\frac{\pi}{4}}}{K\sqrt{\sin\vartheta}}\, e^{i[\Delta_0(\lambda_{12}) + \vartheta_0\lambda_{12}]} \left\{ \sum_{m=1}^{\infty} (-)^m \sum_{n=0}^{\infty} \frac{(-)^n\sqrt{\lambda_n}}{n!\,\xi_n}\, e^{i\lambda_n(2\pi m - \vartheta - \vartheta_0)} \right\}$$

m_0 is equal to 0 or 1, according as $\vartheta < \bar{\vartheta}_0$ or $\vartheta > \bar{\vartheta}_0$, where $\bar{\vartheta}_0$ has been defined in subsect. 2.2, before eq. (2.18). Moreover we have set

$$(3.12''') \quad \Delta_0(\lambda) = 2\delta_1(\lambda) - \varepsilon(\lambda)\left\{\log[i\varepsilon(\lambda)] - 1\right\}$$

and

$$(3.12^{IV}) \quad \xi_n = i\left(\frac{d\varepsilon}{d\lambda}\right)_{\lambda_n}$$

Now comparing (3.12') or (3.12'') with the addends of the sum (2.18) corresponding to p=0, we get the expressions of the decay exponents and of the diffraction coefficients, which result to be related, respectively, to the locations and to the residues of the poles in the

complex-angular-momentum plane. In particular we have

$$(3.13)\qquad D_n^2 = \frac{(-)^n\sqrt{\lambda_n \cos\frac{\vartheta_0}{2}}}{n!\ \xi_n}$$

which, as can be seen from (3.12^{IV}), results to tend to 0 in the limit of $\hbar \to 0$. Both decay exponents and diffraction coefficients can be computed numerically once the potential is known. However, in order to give a rough idea of the dependence of such quantities on the parameters of the potential, it may be useful to use the approximation (3.7) for $\xi(\lambda)$: substituting (3.7) into (3.6), we get

$$(3.14)\qquad \alpha_n \cong (n+\tfrac{1}{2})\frac{r_{12}^2\sqrt{\mu|V_B''|}}{\hbar\,\lambda_{12}};$$

it can be shown that this approximation holds true as long as n is sufficiently small and $r_{12}^2\sqrt{\mu\,|V_B''|}(2\hbar)^{-1} >> 1$, a condition which is frequently met in cases of interest. Similarly we get

$$(3.14')\qquad D_n \cong i^n\left(\frac{\mu}{|V_B''|}\right)^{\frac{1}{4}}\frac{r_{12}\sqrt[4]{\cos\frac{\vartheta_0}{2}}}{e^{i\frac{\pi}{4}}\sqrt[4]{\hbar^2\lambda_{12}}\sqrt{n!}}.$$

3.2. The second term of the Debye expansion.

Let us consider the second term of the series (3.5). Each term (3.5^{II}) corresponding to p=1 can be written as

$$(3.15)\qquad f_m^{1\pm}(k,\vartheta) = \frac{(-)^m}{ik\sqrt{2\pi\sin\vartheta}}\int_0^\infty \lambda^{1/2}\exp\left[i\phi_m^{1\pm}(\lambda,\vartheta)\right]d\lambda,$$

where

$$(3.15')\qquad i\phi_m^{1\pm}(\lambda,\vartheta) = i\left[\phi_m^{0\pm}(\lambda,\vartheta)+2S_{32}\right]-2\pi\varepsilon-\log\left[N(i\varepsilon)\right]$$

and $\phi_m^{0\pm}(\lambda,\vartheta)$ is given by (3.9). The saddle points of this phase are given by

$$(3.16)\qquad \Theta^1(\lambda) = \mp\vartheta - 2m\pi,$$

with

$$(3.16')\qquad \Theta^1(\lambda) = \Theta^0(\lambda)+\vartheta_{32}+\varphi_1+\varphi_2$$

and

(3.16″) $\varphi_2 = 2\pi i d\xi/d\lambda$, $\quad \vartheta_{32} = 2dS_{32}/d\lambda$,

while φ_1 is given by (3.10″). Now it is straightforward to see that $\vartheta_{32}(0) = -\pi$, moreover $\vartheta_{32}(\lambda)$ has a logarithmic cut at λ_{12}, which is exactly compensated by the cut of φ_1 at the same point; therefore the real part of $\Theta_i(\lambda) = [\vartheta_{32}(\lambda) + \varphi_1(\lambda)]$ has the shape represented in fig. 3, with a relative maximum at a $\lambda = \bar{\lambda} < \lambda_{12}$ and a relative minimum close to λ_{12}; the imaginary part of this function is negligibly small for $\lambda_{12} < \lambda < \lambda_{23}$. From these considerations it follows that the real part of $\Theta'(\lambda)$ (see formula (3.16′)) vanishes at $\lambda = 0$ and has a minimum, to be called $-\vartheta_1$, for λ near λ_{12}.

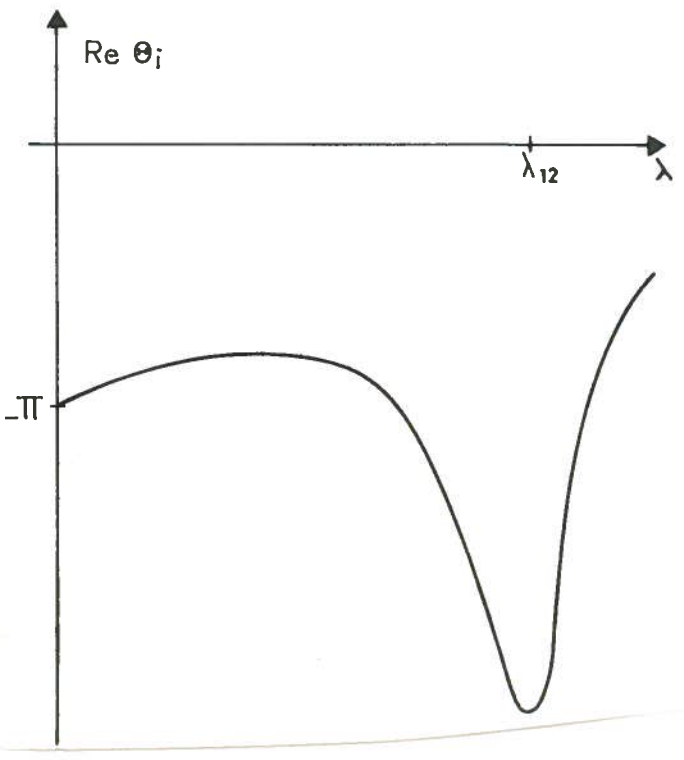

Fig. 3 - Shape of the real part of $\Theta_i(\lambda)$.

As regards the asymptotic evaluation of the second term of the Debye expansion, we observe that, for $\lambda > \lambda_{12}$, the imaginary part of $\Phi_m^{1t}(\lambda, \vartheta)$ increases towards increasing λ, due to decreasing penetration effects; therefore we do not worry about the behavior of the deflection function $\Theta'(\lambda)$ for any real value of λ sufficiently greater than λ_{12}; in particular we neglect the effects of the singularity of $\Theta'(\lambda)$ for $\lambda = \lambda_{23}$, which corresponds to the surface waves that travel from the shadow region to the lit region (see

subsect. 2.2). With this approximation in mind, and proceeding as in subsect. 3.1, we can distinguish between two situations, i.e. $\vartheta'_{\pm} < -\vartheta_1$ and $\vartheta'_{\pm} > -\vartheta_1$. In the former case only the residues of the (second order) poles must be considered. On the contrary in the latter case one has to take into account the contribution of one or, at most, two saddle points: one has a very small imaginary part and a real part less than λ_{12}, the other one gives a negligible contribution for λ sufficiently above λ_{12}, whereas for λ slightly above λ_{12} it has a negative imaginary part; the former saddle point corresponds to a real trajectory of class $K_1^{(a)}$, the latter one (when it is taken into account) corresponds to a trajectory of class $K_1^{(b)}$.

Let us examine in particular the contribution of the poles, which correspond to the surface trajectories that take one shortcut; this contribution is given approximately by

$$(3.17)\quad f_1^{Res}(k,\vartheta) = f_{1+}^{Res}(k,\vartheta) + f_{1-}^{Res}(k,\vartheta),$$

where

$$(3.17')\quad f_{1+}^{Res}(k,\vartheta) = \frac{e^{i(\Delta_1 - \frac{\pi}{4})}}{ik\sqrt{2\pi \sin\vartheta}} \left\{ \sum_{m=m_0}^{\infty} (-)^m \sum_{n=0}^{\infty} \frac{\sqrt{\lambda_n}}{(n!\ \xi_n)^2}\, \zeta_{1m}^{+}\, e^{i\lambda_n \zeta_{1m}^{+}} \right\}$$

$$(3.17'')\quad f_{1-}^{Res}(k,\vartheta) = \frac{e^{i(\Delta_1 - \frac{\pi}{4})}}{ik\sqrt{2\pi \sin\vartheta}} \left\{ \sum_{m=1}^{\infty} (-)^m \sum_{n=0}^{\infty} \frac{\sqrt{\lambda_n}}{(n!\ \xi_n)^2}\, \zeta_{1m}^{-}\, e^{i\lambda_n \zeta_{1m}^{-}} \right\}$$

and

$$(3.17''')\quad \Delta_1 = \Delta_0(\lambda_{12}) + 2S_{32}(\lambda_{12}) + \lambda_{12}\vartheta_1 ;$$

m_0 is equal to 1 for $\vartheta < \bar{\vartheta}_1$ and 0 for $\vartheta > \bar{\vartheta}_1$, where $\bar{\vartheta}_1 = \pm\vartheta_1 \pmod{2\pi}$, $0 < \bar{\vartheta}_1 < \pi$; lastly $\zeta_{1m}^{\pm}$ have been defined by (2.19). (3.17) corresponds to the second term (p=1) of the sum (2.18) relative to the surface-trajectory contribution; the comparison of the two formulae gives as a result the formula of the refraction coefficients for the trajctories which take a shortcut, i.e.

$$(3.18)\quad D_{12}D_{21}(q_f/q_i)^{\frac{1}{2}} = \frac{(-)^n}{n!\sqrt{2\pi}\ \xi_n}\ .$$

This product results to be much less than 1 in the limit of $\hbar \to 0$, as well as the diffraction coefficients.

3.3 The p-th term of the Debye expansion.

As regards the generic p-th term of the series (3.5'), from (3.4') and (3.5'') one gets

$$(3.19)\quad f_m^{p\pm}(K,\vartheta) = \frac{(-)^{m+p+1}}{iK\sqrt{2\pi\sin\vartheta}} \int_0^\infty \lambda^{1/2}\, e^{i\phi_m^{p\pm}(\lambda,\vartheta)}\, d\lambda\,,$$

with

$$(3.20)\quad i\phi_m^{p\pm}(\lambda,\vartheta) = i\phi_m^{0\pm}(\lambda,\vartheta) - 2\pi\varepsilon + ip\left\{2S_{32} + i\log[N(i\varepsilon)]\right\}.$$

The location of the saddle points is given by the equation

$$(3.21)\quad \Theta^p(\lambda) = \mp\vartheta - 2m\pi,$$

where

$$(3.22)\quad \Theta^p(\lambda) = \Theta^0(\lambda) + \varphi_2 + p(\vartheta_{32} + \varphi_1)$$

and ϑ_{32}, φ_2 and φ_1 are given, respectively, by (3.16'') and (3.10''). Reasoning in a way analogous to the case of p=1, it is straightforward to show that $\Theta^p(\lambda)$ is analytical for any real positive value of λ, except at λ_{23}; the real part of $\Theta^p(\lambda)$ has a minimum near λ_{12}, whose value we call $-\vartheta_p$. Moreover $\Theta^p(0) = (1-p)\pi$ and, for sufficiently large values of p, the deflection function presents a rainbow in correspondence of a λ less than λ_{12}, as can be shown observing the shape of the real part of the function $\Theta_i(\lambda)$ (see fig. 3).

As in the case of p=1, for $\vartheta'_\pm < -\vartheta_p$ the asymptotic behavior of integrals (3.19) is determined by the residues at the ((p+1)-th order) poles, whereas for $\vartheta'_\pm > -\vartheta_p$ one has to evaluate the saddle-point contributions. For p>1 the saddle points correspond to complex trajectories of classes $K_p^{(a)}$ or $K_p^{(b)}$, according as $\mathrm{Re}\,\lambda < \lambda_{12}$ or $\mathrm{Re}\,\lambda > \lambda_{12}$. On the other hand the residues at the poles represent the contribution from those surface trajectories which take p shortcuts; among

these we must take into account those which have 1,2,...,p-1 limiting internal reflections (see [5] and[8]); in particular the comparison with the p-th terms of eq.(2.18) gives us the reflection coefficient relative to the shortcuts; this coefficient results to be

(3.23) $R_{22}=\frac{-3\,i}{\sqrt{2\pi}}\,\varsigma(\lambda_n)$,

where

(3.23') $\varsigma(\lambda_n)=\frac{d}{dz}\left[(z+n)\Gamma(z)\right]_{z=-n}$.

This coefficient results to be less than 1, moreover it decreases very rapidly at increasing n; this observation, together with the considerations made about formula (3.18), allows us to conclude that the series (2.18) converges, as we had already said in the preceding section.

4. Remarks.

In this section we make some remarks about some particular effects, like resonances and orbiting, furthermore we outline the case of a complex potential, lastly we draw a brief conclusion.

A) Resonances.

According to our approximation the resonances can be conveniently described by the poles of the S-function, which, owing to (3.3), are determined by the following equation:

(4.1) $\exp(2iS_{22})=-N(i\varepsilon)$;

condition (4.1) is very similar to the one obtained by Knoll and Schaeffer[1]. We have a resonance every time a root of (4.1) approaches a half-integer value; this condition is equivalent to imposing that a point-like particle, which penetrates inside the orbiting sphere, have a large probability amplitude of being reflected many times inside

the sphere (see subsect. 2.2). Such resonances correspond to multiply reflected trajectories inside the sphere Ξ_1 and result to be rather broad for $Re\lambda < \lambda_{12}$ and narrower for $Re\lambda > \lambda_{12}$, similarly to the case of a sharp-edged sphere[8]; a narrow resonance occurs at $\lambda = \lambda_{12}$, if $n_o \vartheta_t = 2\pi$, n_o being a positive integer ($n_o = 3,4,5...$). Überall et al.[7] give a slightly different interpretation of the poles of the S-function, in the sense that they refer to an acoustical model, rather than to trajectories or rays[8].

B) Orbiting and surface waves.

In sect. 3 we have determined the contribution of the surface trajectories and, in particular, the diffraction coefficients and decay exponents relative to them. Now, comparing our expressions with formula (42) of ref.[4], we realize that the orbiting amplitude decreases exponentially towards increasing scattering angles, therefore it represents a wave which is exponentially damped in the direction of propagation, as well as the surface waves; moreover the decay exponent relative to the trajectories with angular momentum $\lambda > \lambda_{12}$ is approximately equal to the decay exponent of the surface wave with the "mode" corresponding to n=0, as can be seen comparing formula (43) of ref.[4] with the expression (3.14). Therefore we can conclude that orbiting behaves in a very similar way to surface waves. The scattering by a nuclear potential is very similar to the scattering by a sharp-edged, charged spherical well[5], since also in the latter case we have "Coulomb" trajectories for $\lambda > \lambda_g$ (where is the "grazing" angular momentum[5]) and surface trajectories for $\lambda = \lambda_g$. All that seems to legitimate the phenomenological model used[5] in order to fit the anomalous backward peaks. Moreover it is worth stressing the importance of the orbiting and

surface wave contribution to the backward scattering amplitude in the case of a weakly absorbing potential: as can be checked from the analysis made in ref.[17], the ^{16}O-^{16}O backward peak is dominated by orbiting; this is in accord with the conclusions of Bosanac[18] about atomic potentials, in contrast with the usual statement that orbiting gives a negligible contribution to the differential cross section[11].

C) Complex nuclear potentials.

Let us consider a complex potential, such that the quantity $E-V_{eff}(r)$ (where V_{eff} is the effective potential) have three and only three turning points for any value of the angular momentum. Then all the saddle points are complex, with an imaginary part more or less large, according to the value of λ and to the intensity of the imaginary part of the nuclear potential. The orbiting angular momentum, λ_{orb}, is pushed into the fourth quadrant of the c.a.m. plane, therefore the surface wave contribution is reduced. Moreover, if the absorption is rather weak (as, e.g., in the examples considered in refs.[2] and[7]), one has to take into account several terms of the Debye expansion: those saddle points which should have a very small imaginary part in the limit of vanishing absorption (see sect. 3) acquire a small imaginary part, but one must keep the same subdivision into angular regions as in the real case. When the absorption increases, the mumber of Debye terms to be considered decreases, whereas the imaginary part of the saddle points increases; moreover the transition from an angular region to another is more and more smoothed off. In the case of very strong absorption only the first Debye term needs be considered; moreover the trajectories which give a contribution to the scattering amplitude are the "Coulomb"

trajectories (at large impact parameters), the "nuclear" trajectories and the surface waves (which, as we have seen, behave in a very similar way) and the directly reflected trajectories; an alternative description of this situation is given in ref.[14].

D) Further developments.

We conclude with two remarks on possible developments of the present theory. At first we observe that the formulae deduced in the present paper are not valid in the limit of very small diffusenesses; in this connection we recall that in some realistic cases the approximation of refs.[1] and [2] fails; if one could write a suitably approximate S-function for the case of a very small diffuseness, of course a more general expression of the decay exponents and of diffraction coefficients would be obtained. Secondly we note that the treatment now followed could be applicable, in analogy to what has been done in the case of optics[9], also to the case of non-central potentials, which vary rapidly in some regions of the space: in fact, due to the localization principle, the diffraction coefficients, as well as the decay exponents and the reflection and refraction coefficients, depend only on the local properties of the interaction region.

ACKNOWLEDGEMENTS

The author is thankful to his friends profs. M. Giannini and G. Passatore for useful and stimulating suggestions and discussions.

Appendix

We prove that the scattering amplitude, as written in the approximation by Brink and Takigawa[2], can be expanded according to (3.5). To this end we must establish some preliminary results about the action integrals introduced in (3.3). Moreover we study the deflection function $\Theta^{\circ}(\lambda)$ and the function $N(i\varepsilon)$.

In particular we are interested in the integrals

(A.1) $S_1 = A(r_1, R)$, $S_{21} = A(r_2, r_1)$, $S_{32} = A(r_3, r_2)$, $S_3 = A(r_3, R)$,

where $A(r,r')$ is defined by (3.3″) and $R \gg r$. One has

(A.2) $S_3 = S_{32} + S_{21} + S_1$.

The situation is different according to the value of λ considered; in particular let us distinguish among the cases i) $\lambda < \lambda_{12}$, ii) $\lambda_{12} < \lambda < \lambda_{23}$, iii) $\lambda > \lambda_{23}$.

i) $\lambda < \lambda_{12}$

Since $r_2 = r_1^*$, r_3 is real and the integrand of (3.3″) is real on the real axis, by Schwartz's reflection principle one has

(A.3) $A^*(r_3, r_2) = A(r_3, r_1)$;

moreover

(A.4) $A(r_3, r_1) = A(r_3, r_2) + A(r_2, r_1)$,

whence, by (A.3), one gets

$$A^*(r_3, r_2) - A(r_3, r_2) = A(r_2, r_1),$$

i.e.

(A.5) $A(r_2, r_1) = -2i\,\mathrm{Im}[A(r_3, r_2)]$;

therefore $A(r_2, r_1)$ is purely imaginary. Furthermore, one has, from (3.3′),

(A.6) $S_{21} = i\pi\varepsilon(\lambda)$;

now it is straightforward to see that ε is real and negative for $\lambda < \lambda_{12}$ (see formula (3.7)). Then from (A.5) and (A.6) we get

(A.7) $-2\,\mathrm{Im}S_{32} = \pi\varepsilon(\lambda) < 0$.

Furthermore, since r_3 is real, also S_3 is real. Then by

(A.2) we get

$$ImS_{32}+ImS_{21}+ImS_{1}=0,$$

whence, by (A.6) and (A.7), one obtains

(A.8) $ImS_{32}=ImS_{21}=-\frac{1}{2}ImS_{21}>0.$

Using a quite analogous argument, we can conclude that $Im[\Theta^{\circ}(\lambda)]<0$ for $\lambda<\lambda_{12}$.

ii) $\lambda_{12}<\lambda<\lambda_{23}$

In this case S_1 and S_{32} are real, so (A.2) implies that

(A.9) $ImS_3=ImS_{21}=\Pi\xi>0;$

the last relation follows from (A.6) and from the reality of $\xi(\lambda)$ for λ less than λ_{23}.

iii) $\lambda>\lambda_{23}$.

In this case, owing to the fact that the integrand of (3.3) is purely imaginary on the real axis, Schwartz's reflection principle implies

$$(-iS_{21})^{*}=-iS_{31},$$

where $S_{31}=A(r_3,r_1)$; then

$$S_{21}^{*}=-S_{31}.$$

Moreover

$$S_{31}=S_{32}+S_{21};$$

from the above formulae it follows that

(A.10) $S_{32}=S_{31}-S_{21}=-S_{21}^{*}-S_{21}=-2ReS_{21}.$

This proves that S_{32} is purely real on the real axis; then

(A.11) $ImS_3=ImS_{21}.$

Moreover, using arguments very similar to those which led to the determination of the sign of ξ in a neighborhood of λ_{12} (see ref.[2]), we conclude that S_{32} is negative for $\lambda>\lambda_{23}$, so that $ReS_{21}>0$ and, by definition (see formula (3.3')),

(A.12) $Im\xi<0.$

Now we are ready to prove that the scattering amplitude (3.3) can be written as a geometric series, say (3.4), for any real positive value of λ. The proof will be complete if we show that

(A.13) $|\exp(2iS_{32})|<|N(i\varepsilon)|$

for any real positive λ. Let us consider two different cases: i) $\lambda \leq \lambda_{23}$, ii) $\lambda > \lambda_{23}$. In the former case ε is real; then, by Schwartz's reflection principle,

(A.14) $\Gamma^{*}(\frac{1}{2}+i\varepsilon)=\Gamma(\frac{1}{2}-i\varepsilon)$.

Furthermore

(A.15) $\log(i\varepsilon)=\log|\varepsilon|+i\frac{\varepsilon}{|\varepsilon|}\frac{\pi}{2}$.

Then, taking into account (A.15) and the properties of the gamma function, we get

(A.16) $|N(i\varepsilon)|^2=1+\exp(-2\pi|\varepsilon|)>1$.

Since, as we have seen, $\mathrm{Im}S_{32}\geq 0$ for $\lambda<\lambda_{23}$, from (A.16) it follows (A.13). Vice versa, for $\lambda>\lambda_{23}$, we assume - in accord with Brink's approximation - that r_1 is sufficiently far from r_2, so that $|\varepsilon|>>1$. Then, using Stirling's formula, one has

(A.17) $N(i\varepsilon)\cong\exp\left\{\frac{1}{2}-i\varepsilon\left[\log\left(1+\frac{1}{2i\varepsilon}\right)\right]\right\}$;

furthermore, developing the logarithm in (A.17) up to second order in ε, we have

(A.18) $|N(i\varepsilon)|\cong\exp[-\mathrm{Im}\varepsilon/(8|\varepsilon|^2)]$.

On the other hand we have shown that for $\lambda>\lambda_{23}$ $\mathrm{Im}\varepsilon<0$ and S_{32} is purely real; then (A.13) is proved also for $\lambda>\lambda_{23}$. Incidentally (A.18) (which holds true as long as λ does not belong to the region H_0 of the complex λ-plane) implies that $N(i\varepsilon)$ is nearly 1 for λ outside H_0.

However, since for $\lambda\to\infty$ $|\varepsilon|\to\infty$, from (A.18) it follows that $|e^{2iS_{32}}/N(i\varepsilon)|\to 1$ as $\lambda\to\infty$. Therefore we have still to prove that each integral (3.2) can be interchanged with the series (3.4). To this end we proceed in a similar way to ref.[8], i.e. we split integrals (3.2) into two terms,

(A.19) $$\int_0^{\infty} d\lambda = \int_0^{\Lambda} d\lambda + \int_{\Lambda}^{\infty} d\lambda .$$

Now in the former addend of (A.19) the series can be interchanged with the integral, since it converges uniformly for any λ between 0 and Λ. As for the latter addend, after the substitution of (3.4) into the integral (3.2), we have

$$\text{(A.20)}\quad \int_{\Lambda}^{\infty} \lambda^{1/2} S(\lambda,K)\, e^{i\left[2\pi m\lambda \pm \left(\lambda\vartheta - \frac{\pi}{4}\right)\right]} d\lambda = \int_{\Lambda}^{\infty} \lambda^{1/2} \sum_{p=0}^{\infty} S_p(\lambda,K)\, e^{i\left[2\pi m\lambda \pm \left(\lambda\vartheta - \frac{\pi}{4}\right)\right]} d\lambda\ ;$$

but the terms of the series which appears in the integrand of r.h.s of (A.20) are exponentially small for $p>0$ and Λ sufficiently large. Therefore the series can be interchanged with the integral.

REFERENCES

[1] J. Knoll and R. Schaeffer: Ann. Phys. (N.Y.), 97, 307 (1976)

[2] D. M. Brink and N. Takigawa: Nucl. Phys. A, 279, 159 (1977)

[3] M. V. Berry and K. E. Mount: Rep. Prog. Phys., 35, 315 (1972)

[4] K. W. Ford and J. A. Wheeler: Ann. Phys. (N. Y.), 7,259 (1959)

[5] E. Di Salvo and G. A. Viano: Nuovo Cim. A, 59, 11 (1980); 71, 261 (1982); 80, 317 (1984); E. Di Salvo: Nuovo Cim. A, 74, 427 (1983)

[6] R. C. Fuller: Nucl. Phys. A, 216, 199 (1973)

[7] H. Uberall, A.Farhan, O.Dragun and E. Maqueda: Nuovo Cim. A, 57, 205 (1980); Nucl. Phys. A, 362, 241 (1981)

[8] H. M. Nussenzveig: Journ. Math. Phys., 10, 125 (1969)

[9] J. B. Keller: Proc. Symp. Appl. Math., 8, 27 (1958); B. R. Levy and J. B. Keller: Commun. Pure Appl. Math., 12, 159 (1959)

[10] R.Anni and L. Renna: Nuovo Cim. A, 65, 311 (1981)

[11] B. J. B. Crowley: Phys. Lett. A, 71, 186 (1979); 75, 183 (1980); Phys Rep., 57, 48 (1980)

[12] R. Courant: "Methods of Mathematical Physics", Vol. 2 (New York, N. Y., 1962), pag 79.

[13] L. Landau and E. Lifchitz: "Mecanique Quantique" (Moscow, 1966), p. 217

[14] E. Di Salvo: to be published on Nuovo Cim. A

[15] E. Di Salvo: Lett. Nuovo Cim., 42, 49 (1985)

[16] M. V. Berry: Proc. Phys. Soc., 89, 479 (1966)

[17] S. Y. Lee, N.Takigawa and C. Marty: Nucl. Phys. A 308, 161 (1978)

[18] S. Bosanac: Phys. Rev. A 19, 125 (1979)